Bioconjugate Chemistry

Article

pubs.acs.org/bc

Rational Design of Chemical Ligands for Selective Mitochondrial Targeting

Silvie Rimpelová,[#] Tomáš Bříza,[§,∥] Jarmila Králová,[†] Kamil Záruba,[§] Zdeněk Kejík,[§,∥] Ivana Císařová,[‡] Pavel Martásek,[∥] Tomáš Ruml,*[,#] and Vladimír Král*[,§,⊥]

[#]Department of Biochemistry and Microbiology and [§]Department of Analytical Chemistry, Institute of Chemical Technology in Prague, Technická 5, 166 28, Prague 6, Czech Republic

[∥]Department of Pediatrics and Adolescent Medicine, First Faculty of Medicine, Charles University in Prague, Kateřinská 32, 121 08, Prague 2, Czech Republic

[†]Institute of Molecular Genetics, Academy of Science of the Czech Republic, Vídeňská 1083, 142 20, Prague 4, Czech Republic

[‡]Department of Inorganic Chemistry, Faculty of Science, Charles University in Prague, Hlavova 2030/8, 128 43, Prague 2, Czech Republic

[⊥]Zentiva Development (part of Sanofi group), U Kabelovny 130, 102 37, Prague 10, Czech Republic

Supporting Information

ABSTRACT: The rational design of molecules with selective intracellular targeting is a great challenge for contemporary chemistry and life sciences. Here, we demonstrate a rational approach to development of compartment-specific fluorescent dyes from the γ-aryl substituted pentamethine family. These novel dyes exhibit an extraordinary affinity and selectivity for cardiolipin in inner mitochondrial membrane and possess excellent photostability, fluorescent properties, and low phototoxicity. Selective imaging of live and fixed mitochondria was achieved in various cell lines using nanomolar concentrations of these dyes. Their high localization specificity and low toxicity enables study of morphological changes, structural complexity, and dynamics of mitochondria playing a pivotal role in many pathological diseases. These far-red emitting dyes could also serve in a variety of biomedical applications.

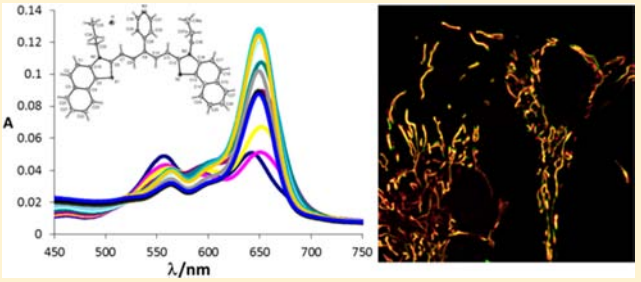

INTRODUCTION

The requirement of fluorescent probes[1,2] for live cell imaging initiated a boom in the development of small organic molecules.[3,4] One group of such dyes are cyanines (methine salts, MS), of which absorption wavelengths can be tuned by a number of vinylene moieties[5] in a conjugated system. MS have multiple uses[6−18] and gained additional popularity in single molecule fluorescence microscopy.[19] Pentamethine and heptamethine derivatives are promising candidates for clinical applications[20] due to their absorption in far-red and near-infrared wavelength regions, emission of ∼700−1000 nm, high extinction coefficients,[21] and high fluorescence quantum yields.[22] Notably, γ-aryl substituted MS are described rarely in the literature,[23,24] which opens an opportunity to reveal new fluorescent subcellular probes and sensors.

Selective receptors for biologically important anions have been a focus of our group for the past decade. We achieved enhanced selectivity of oxoanions for porphyrin-based receptors[25] and published the first preparation of chromophoric binaphthyl derivatives,[26] double chromophoric porphyrin−pentamethine conjugates,[27] as well as developed selective sulfate receptors based on substituted γ-aryl pentamethine scaffold.[24] In addition, we have proven their application as optical sensors for heparin and other sulfated and phosphate anions.[24] This finding directed our interest to explore whether pentamethine salts could specifically interact with 1,3-bis(*sn*-3′-phosphatidyl)-*sn*-glycerol [cardiolipin, CL][28] in inner membrane of mitochondria to enable their imaging.

Monitoring of mitochondria by vital fluorescent dyes is a desirable task, as these organelles are major energy suppliers and represent an important intersection between cell life and death. Generally, mitochondria are usually monitored by vital fluorescent dyes, as other methods, including Nomarski contrast or electron microscopy, are not always suitable. Most fluorescent dyes accumulating in mitochondria are lipophilic cations.[29] Conventional mitochondrial dyes include tetramethylrhodamine methyl ester and ethyl ester (TMRM and TMRE, respectively), DiOC6(3) [3,3-dihexyloxacarbocyanine iodide], and JC-1 [5,5′,6,6′-tetrachloro-1,1′,3,3′-tetraethylbenzimidazolylcarbocyanine iodide].[30] In spite of the fact that these fluorescent dyes are widely used, their general applicability is in some respects limited and requires careful selection. Some dyes

Received: October 18, 2012
Revised: July 2, 2013
Published: August 20, 2013

are substrates of multidrug resistant protein (P-glycoprotein), and staining profiles depend on its activity.[31] Moreover, they are easily released during fixation, as their mitochondrial retention depends on membrane potential. The other issues might be (i) low specificity (e.g., rhodamine 123 stains besides mitochondria also endoplasmic reticulum [ER] and Golgi apparatus);[32] (ii) inhibition of mitochondrial respiration [e.g., DiOC6(3),[29] TMRM, and TMRE[35]]; (iii) redistribution into ER;[33] (iv) dual emission spectra (JC-1,[34] MitoCapture[32]) preventing multicolor imaging in colocalization studies; (v) photobleaching (MitoTracker probes based on cyanine dyes containing a thiol-reactive moiety, e.g., MitoTracker Green FM [MTG]).[35]

The only reported probe binding to mitochondrial CL has been NAO (10-*N*-nonyl acridine orange). However, it is not suitable for multicolor labeling, since it shifts from a green fluorescent monomeric form [abs./em. 495/519 nm] to a dimeric form exhibiting red fluorescence [emission shift to 640 nm[36]]. For these reasons, it is obvious that there is a need for novel mitochondria-specific sensors to extend application possibilities and enable greater flexibility.

Generally, to achieve specific intracellular targeting requires the following: (i) knowledge of organelle specific binding site (e.g., identification of membrane receptors), (ii) design of proper molecules (probes) with selective binding ability for selected subcellular target, (iii) assaying binding selectivity, and (iv) proper balance of lipophilicity/hydrophilicity and charge. The almost exclusive incidence of CL in the inner mitochondrial membrane of mammalian cells makes it a perfect target for mitochondria-specific probes. Therefore, we have strived to develop such a new class of vital probes specific for mitochondrial CL based on selective molecular recognition mediated by pentamethine salts. For this purpose, we have prepared various γ-aryl substituted pentamethine salts and tested them as receptors for phospholipidic CL according their binding affinity. Their photophysical and biological properties were determined, and herein we present data demonstrating feasibility of our approach by generating dyes with superior performance for mitochondrial imaging in comparison to commercial probes, and suggesting further potential applications.

EXPERIMENTAL PROCEDURES

Chemicals. Unless otherwise indicated, common reagents or materials were obtained from commercial source and used without further purification. Chemicals for preparation of compounds **1**−**5** were purchased from Sigma Aldrich. Aromatic malondialdehydes were purchased from Acros Organics. Cy5 NHS ester and compound **6** were purchased from Lumiprobe and Sigma Aldrich, respectively. All details about properties of these dyes are available at websites of the companies. Bovine heart solution of CL in ethanol was purchased from Sigma Aldrich.

*Synthesis of **1** and **2**.* Benzeneacetaldehyde, 4-nitro-α-[2-(3-propyl-2(3*H*)-benzo-thiazolylidene)ethylidene] (compound **1**) and benzothiazolium, 2-[3-(4-nitrophenyl)-5-(3-propyl-2(3*H*)-benzo-thiazolylidene)-1,3-pentadien-1-yl]-3-propyl-, iodide [1:1] (compound **2**) syntheses have been already published by our group,[37,24] respectively. Structures of these compounds are depicted in Scheme S1.

*Synthesis of **3**.* α-Naphthothiazolium, 2-[(1*E*,3*Z*,5*Z*)-3-(pyrimidine)-5-(3-propyl-2(3*H*)-α-naphthothia-zolylidene)-1,3-pentadien-1-yl]-3-propyl-, iodide [1:1] (compound **3**) synthesis is described in this paragraph. The flask was charged with 2-(4-pyridyl)malondialdehyde (75 mg, 0.50 mmol), 2-methyl-3-propyl α-naphthothiazolium iodide (373 mg, 10.1 mmol), and dry *n*-butanol (10 mL). The mixture was stirred at 110 °C for 18 h. After cooling to laboratory temperature, the mixture was filtered and the solid part was washed with ethanol (3 × 5 mL) and dried in vacuum. Product **3** was obtained as a green-brown powder, 302 mg, 83%. Structure of compound **3** is depicted in Scheme S1. ^{1}H NMR: 8.98 (2H, d, J = 5.6 Hz), 8.2−7.9 (12H, m), 7.80 (2H, t, J = 7.3 Hz), 7.67 (2H, t, J = 7.5 Hz), 6.36 (2H, d, J = 11.6 Hz), 4.45 (4H, t, J = 6.5 Hz), 1.78 (4H, sextet, J = 7.2), 0.94 (6H, t, J = 7.3 Hz). ^{13}C NMR: 165.6, 140.2, 130.8, 130.1, 129.8, 129.4, 127.5, 126.6, 123.5, 122.1, 113.8, 48.5, 21.9, 11.3. HRMS for $C_{38}H_{34}IN_3S_2$ calculated: 596.2189 (M^+), found: 596.2184 (M^+). Elementary analysis for $C_{38}H_{34}IN_3S_2$ calculated: C 63.06%, H 4.74%; found: C 63.11, H 4.80. X-ray crystals were obtained by crystallization from ethanol at room temperature.

*Synthesis of **4**.* Benzothiazolium, 2-[3-(pyrimidine)-5-(3-propyl-2(3*H*)-benzothiazolylidene)-1,3-pentadien-1-yl]-3-propyl-, iodide [1:1] (compound **4**) synthesis is described below. The flask was charged with 2-(4-pyridyl)malondialdehyde (150 mg, 1.00 mmol), 2-methyl-3-propyl benzothiazolium iodide (640 mg, 20.1 mmol), and dry *n*-butanol (25 mL). The mixture was stirred at 110 °C for 18 h. After cooling to laboratory temperature, the mixture was filtered; the solid part was washed with ethanol (3 × 5 mL) and dried in vacuum. Product **4** was obtained as a green powder, 498 mg, 79%. Structure of compound **4** is shown in Scheme S1. ^{1}H NMR: 8.94 (2H, d), 8.14−7.80 (8H, m), 7.58 (2H, t), 7.45 (2H, t), 6.20 (2H, d), 4.28 (4H, bs), 1.71 (4H, m), 0.85 (6H, t). ^{13}C NMR: 156.9, 148.2, 143.6, 141.3, 128.2, 127.0, 125.6, 125.5 123.2, 114.0, 98.3, 47.5, 20.9, 10.9. HRMS for $C_{30}H_{32}IN_3S_2$ calculated: 496.1876 (M^+), found: 496.1873 (M^+). Elementary analysis for $C_{30}H_{32}IN_3S_2$ calculated: C 57.59%, H 5.16%, found: C 57.86%, H 4.93%.

*Synthesis of **5**.* Benzothiazolium, 2-[3-(*N*-methyl-pyridimium)-5-(3-propyl-2(3*H*)-benzothiazolylidene)-1,3-pentadien-1-yl]-3-propyl-, iodide [1:1] (compound **5**) synthesis is described in this paragraph. The flask was charged with cyanine dye (55 mg, 88 μmol), DMF (5 mL), and excess of methyliodide (0.5 mL, 2 M solution in t-BuOMe). The mixture was heated in high pressure ampule to 60 °C for 20 h. After cooling, the excess of methyliodide was removed with stream of nitrogen and the rest of the solvent was evaporated. The solid fraction was macerated with diethyl ether and filtered. Obtained solid was crystallized from hot ethanol. Product **5** was formed as a metallic brown powder, 63 mg, 94%. Structure of compound **5** is depicted in Scheme S1. ^{1}H NMR: 8.96 (2H, d), 7.98−8.16 (6H, m), 7.60 (2H, t), 7.48 (2H, t), 6.32 (2H, d), 4.35 (7H, bs), 1.72 (4H, sextet), 0.85 (6H, t). ^{13}C NMR: 166.4, 153.4, 147.9, 145.3, 141.4, 128.3, 127.8, 125.8, 125.7, 123.3, 114.2, 98.6, 47.6, 47.0, 21.1, 10.9. HRMS for $C_{31}H_{35}I_2N_3S_2$ calculated: 255.6053 (M^{2+}), found: 255.6051 (M^{2+}). Elementary analysis for $C_{31}H_{35}I_2N_3S_2$, calculated: C 48.51%, H 4.60%, found: C 48.62%, H 4.56%.

Determination of the Absorption Spectra and Coefficients of MS. Dependence of absorption on the concentration for tested probes **1**−**5** were observed in dimethyl sulfoxide (DMSO), methanol (MeOH), and 1 mM phosphate buffer (H_2O:DMSO, 98:2, v/v) at pH 7.3. Plastic cuvettes with optic length 1 cm were used for measurements of absorption spectra. Concentrations of the salts varied in the range from 0

to 10 μmol L^{-1}. Absorption spectra were obtained on a UV−vis spectrophotometer (Cary 400, Varian; USA) at room temperature. Molar absorption coefficients were calculated using their maximum absorbance by linear regression with program Microsoft Excel 2010.

Fluorescence Emission Spectra Measurement of MS. Fluorescence emission spectra of **2**−**5** were collected using a Fluoromax 2 spectrofluorometer in the DMSO, MeOH, and 1 mM phosphate buffer (H_2O:DMSO, 98:2, v/v) at pH 7.3 at room temperature. Whole fluorescence emission spectra of compounds **2**−**5** could not be measured because the wavelengths of their emission and excitation maxima partially overlap. Therefore we measured only parts of their spectra. Low fluorescence intensity of compound **1** did not allow measurement of its fluorescence emission spectra.

Determination of Quantum Yield of MS 2−5. For the determination of quantum yield (Φ) of MS **2**−**5**, compound **6** was used as a standard. Samples of the MS were prepared from stock solutions to reach absorbance lower than 0.04 at λ_{max} (to prevent the inner filter effect in fluorescence measurement). The emission spectra of the MS **2**−**5** were measured at their excitation maxima. For measurement of emission spectra of standard **6**, the excitation maxima of studied MS **2**−**5** were applied. For both sets of MS, the area under each fluorescence emission curve was calculated and corrected for the Rayleigh peak area (if necessary). The average fluorescence emission peak areas were then calculated for each sample. The relative fluorescence quantum yields were calculated using the following equation: $\Phi_x = \Phi_s \, F_x/F_s/A_x{\cdot}A_s/n_s{\cdot}n_x$, where Φ represents quantum yield, F stands for integrated area under the corrected fluorescence emission spectrum, A is absorbance at the excitation wavelength, n is refractive index of the used solvents, and the subscripts "x" and "s" refer to the unknown and the standard, respectively. Quantum yields of MS **2**−**5** were determined in DMSO, in MeOH, and in water environment represented by PBS, pH 7.3.

Determination of *in Vitro* Photostability of MS. Methine salts were dissolved in DMSO (0.145 mM). According to their absorption coefficient, appropriate amount of DMSO solution was added in phosphate buffer saline (PBS) in 1 cm plastic cuvette. Replicates were prepared as follows: two solutions were prepared—the first was kept in the dark; the second was illuminated with a 150 W halogen lamp with an edge-pass filter (Panchromar, Germany) that transmitted light at wavelengths 500 nm and longer. The fluency rate at the level of the solution in cuvette was 5 mW cm^{-2}. Absorption spectra of both solutions (illuminated and in the dark) were collected (Cintra 404, GBC Scientific) after 10, 20, and 30 min (corresponding total light doses were 3.6 and 9 J cm^{-2}). The percentage of original absorbance at absorption maximum was calculated as the mean of two replicates. For comparison, several commercially available dyes with corresponding structural backbone [compound **6** (pentamethine benzothiazole derivative $DiSC_3(5)$ and Cy5 (pentamethine indole derivative)] or mitochondria-specific [MitoTracker Deep Red FM (MT)] were used.

Determination of the Conditional Constants of MS with Cardiolipin and Phosphatidylserine. The association of the salts **1**−**5** and standards **6**, Cy5, and MT with tested analytes (CL and phosphatidylserine [PS]) was studied by means of UV−vis spectroscopy in a phosphate buffer (0.001 M, water:DMSO, 98:2, v/v) at pH 7.3. Conditional constants (Ks) were calculated from the absorbance changes of the salts using absorbance maximum of their complexes (ΔA) by nonlinear regression with program Letagrop Spefo 2005. The wavelength of the used absorbance maxima for salts **1**−**6**, Cy5, and MT were 497, 648, 690, 649, 633, 657, 648, and 648 nm, respectively. The error of the measurement was expressed as three times the standard deviation between the measured data and calculated curve. Concentration of the used salts was 4.7 μmol L^{-1}; concentration of the studied analytes was in the range 0−0.5 mmol L^{-1}.

In vitro cell techniques used and studies are described in Supporting Information.

RESULTS AND DISCUSSION

Synthesis of γ-Aryl Substituted Symmetrical MS. Here, we describe the design, synthesis, and application of three types of dyes: a neutral merocyanine **1**, charged symmetric γ-aryl substituted methine salts **2**−**4**, and doubly charged salt **5** (all shown in Figure 1, Supporting Information Scheme S1, Figures

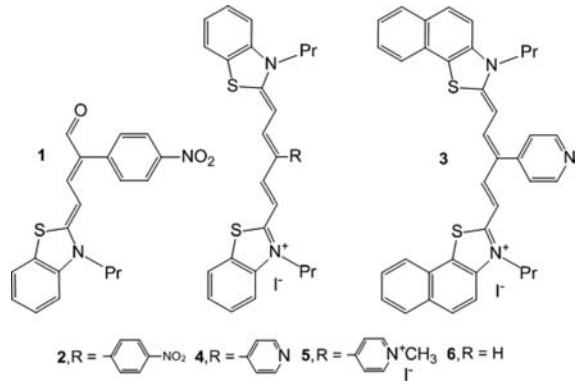

Figure 1. Mitochondrial probes based on γ-aryl substituted MS. Neutral merocyanine **1**, salts **2**−**4**, salt **5** (quarternized to the second stage), and salt **6** (a non-γ-aryl substituted derivative).

S1). Details of the synthesis are based on our previously published methodology.[24,37] The chemical structures and characterizations by ^{1}H NMR, ^{13}C NMR, and high resolution mass spectroscopy (HRMS) are shown in Supporting Information (Figures S2−S10). In principle, the synthesis is based on condensation of aromatic malondialdehydes and aromatic thiazolium salts. Chemical structure of commercially available MS derivative **6** and Cy5, used here for comparison, are shown in Figures 1 and S11, respectively. The X-ray structure of **3** is represented by Figure 2 (see details in Supporting Information in Materials and Methods, Figure S12).

Photophysical Properties of MS. Spectral properties of MS in DMSO, MeOH, and PBS were determined using UV−vis absorption and fluorescence spectroscopy. The MS were in the monomeric forms in hydrophobic environment (DMSO, MeOH) and in the aggregated forms in aqueous solution. The absorption maxima of monomeric forms of **2**−**5** ranged between 645 and 686 nm and fluorescence emission maxima between 665 and 707 nm (Figure S13, Table S1). The γ-aryl substitution of **6** did not significantly influence λ_{max} of monomeric, monocationic MS **2** and **4** in the aprotic DMSO (about 656 nm). In the MeOH this γ-aryl substitution shifted the λ_{max} from 654 to 645 nm. A comparison of λ_{max} of **3**, **4**, and **5** indicates, that increased charge density of **4** evoked a blue shift of about 10 nm, while the monomeric form of MS **3** displayed the absorption maxima 686 nm in DMSO and 676

dx.doi.org/10.1021/bc400291f | Bioconjugate Chem. 2013, 24, 1445−1454

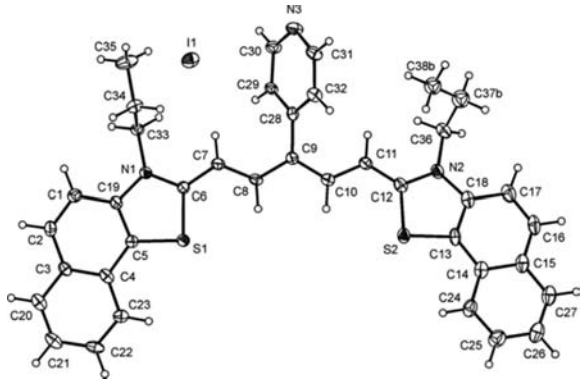

Figure 2. X-ray view of the compound **3** with atom numbering scheme.

nm in MeOH. In this context, it should be mentioned that the region of the lowest absorption coefficient of living tissues and cells is about 700 nm,[38] where our MS are applicable. Absorption and emission maxima of commercial probe, MT, which was developed for this spectral region, are 644 and 664 nm, respectively. Other used mitochondrial probes such as JC-1 and DiOC6(3) have absorption maxima at about 490 and 480 nm, respectively. Their emission maxima are between 500 and 600 nm. With the exception of MS **5**, the absorption maxima of the MS H-aggregates were between 450 and 600 nm and their absorption coefficients were several times lower compared to their monomeric forms. The wavelength of absorption maxima and absorption coefficient of MS **5** H-aggregate was nearly of its monomeric form. This difference likely arose from significantly higher hydrophilicity of MS **5**. Similar behavior was observed for hydrophilic MT and Cy5 probes. Thus, MS spectral properties can be simply and effectively used for recognition of hydrophobic matrix such as cell membrane. Low fluorescence intensity of neutral merocyanine **1** prevented measurement of its fluorescence emission spectra (absorption maxima at 476 nm). For details see Supporting Information (Figure S13, Table S1).

The fluorescence quantum yields of MS **2**–**5** (summarized in Table 1) were determined by using compound **6** as a standard,

Table 1. Quantum Yields of Methine Salts

	quantum yield					
solution	**1**	**2**	**3**	**4**	**5**	**6**
DMSO	[a]	0.02	0.30	0.15	0.15	0.45
MeOH	[a]	0.05	0.27	0.17	0.09	0.36[b]
PBS	-	0.02	0.10	0.11	0.12	0.14

[a]The value of Φ for MS **1** was not calculated because its fluorescence intensity was too low for measuring its fluorescence spectra. [b]Value taken from Bilmes et al.[39]

with Φ of 0.36 in MeOH.[39] Measured Φ of γ-aryl substituted MS **2**–**5** in MeOH was 0.05, 0.27, 0.17, and 0.09, respectively. Our results reveal that the γ-aryl substitution of pentamethine salts strongly affects the Φ value, especially of **2** and **5**. Similarly, it was reported that the γ-aryl substitution can strongly reduce the Φ of Cy5 derivatives (1/3 origin of Cy5).[40] The authors found that this reduction of fluorescence intensity was caused by rotation of the substituted groups. The rotation or vibration of bulky substituents can change the geometry of the molecule in the excited state. These phenomena permit the molecule in the excited state to relax by a nonradiative process, thus reducing its quantum yield. Significant differences among the Φ of MS **2**–**5** and MS **6** are probably caused by rotation of their aromatic substituents at the meso-position of the pentamethine chain. However, more viscous surroundings can effectively suppress these nonradiative transitions of molecules and increase the Φ of probe.[40] It is well-known that viscosity of inner mitochondrial membrane is much higher than of mitochondrial matrix or extra-matrix surroundings.[41] Thus, γ-aryl substitution of pentamethine salts represents a promising modification suitable for design of mitochondria-targeted probes allowing more precise labeling of inner mitochondrial membrane.

The low fluorescence emission intensity of **2** was probably also caused by its fluorescence quenching due to the presence of a substituted nitro group. The results are indicative of a correlation between electron density of MS **3**–**5** and their Φ value. MS **5** with two cationic charges exhibited Φ value approximately one-third of the monocationic MS **4.** Naphthothiazolium MS **3** displayed significantly higher Φ than benzothiazolium MS **4**. On the other hand, the Φ of 4,5:4′5′-dibenzo-3,3,3′,3′-tetramethylindadicarbocyanine does not significantly differ from the value of Φ of the origin of Cy5 (about 0.2 for MeOH).[42]

Values of Φ of MS **2**–**5** and **6** obtained in water environment (1 mM PBS, pH 7.3; see Table 1) were 0.02, 0.10, 0.11, 0.12, and 0.14, respectively. These values, except of Φ of hydrophilic MS **5**, are significantly lower when compared to the values determined in MeOH surrounding. We suppose that formation of aggregates of the dyes occurred in water environment, which limits application of the tested dyes in water. Nevertheless, this fact can lead to enhanced effectiveness of membrane staining.

In vitro photostabilities of compounds **1**–**6** and Cy5 were evaluated in the dark and after exposure to the light of wavelengths longer than 500 nm. The photostabilities were evaluated in DMSO, thus representing the monomeric state of the dyes (see Supporting Information Table S2) and in PBS at different pH values: 4.8, 7.0, and 9.3 (details are given in Table 2). The amounts of residual MS derivatives in PBS after 30 min of light exposure are expressed in percentage. Complete photostability absorption spectra of **1**–**5** as well as **6**, Cy5, and MT were chosen as reference (not shown, but can be provided upon request). The majority of novel polymethine salts were photostable in DMSO and PBS. Their photostability significantly exceeded that of **6** and was comparable to that of Cy5 and MT (Table 2 and Table S2).

In PBS, however, the neutral merocyanine **1** decomposed either in dark or after illumination, thereby correlating with reports for other merocyanine dyes[43] exhibiting their limited usage due to rapid degradation under light. Photostability of salt **2** was strongly affected by the interaction with chloride ions (from PBS) resulting in the increment of absorption maximum. This phenomenon is currently under further investigation for potential exploitation in chloride ions sensing. Compounds **4** and **5** displayed excellent pH and photostability in PBS in contrast to a dye of similar structure but without γ-aryl substitution [MS **6** based on benzothiazolium unit $DiSC_3(5)$]. When compared to Cy5 and MT (pentamethines based on indole ring without γ-aryl substitution), compound **4** exhibited slightly better photostability and MS **5** comparable stability. The stability of MS **4** and **5** was not significantly influenced by pH. Therefore, a significant improvement of MS photostability by γ-aryl substitution has been achieved. Such a strategy could

Table 2. *In Vitro* Photostability of Methine Salts in PBS[a]

		compound depletion[b]							
pH		1	2	3	4	5	6	Cy5	MT
4.8	L[c]	46%	[e]	38%	89%	84%	14%	88%	60%
	D[d]	58%	-	90%	98%	100%	60%	98%	94%
7.0	L	57%	-	45%	97%	83%	14%	86%	86%
	D	66%	-	79%	100%	100%	78%	94%	93%
9.3	L	70%	-	44%	89%	81%	9%	90%	81%
	D	46%	-	95%	97%	100%	64%	99%	91%

[a]Percentage of absorbance at absorption maximum after 30 min incubation in phosphate buffer saline at various pH. [b]Error ±5%. [c]Light (L). [d]Dark (D). [e]Absorption maximum of MS **2** was strongly affected by the interaction with chloride ions (from PBS).

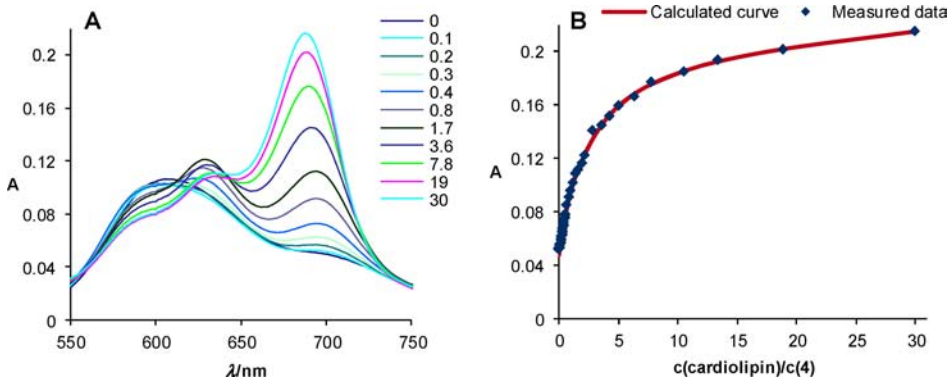

Figure 3. (A) Absorption spectra of the salt **3** (4.7 μM) with cardiolipin in a solution of 1 mM PBS [H_2O:DMSO, 98:2, v/v], pH 7.3. (B) Titration curve of salt **3** (4.7 μmol) in the presence of cardiolipin at 690 nm.

Table 3. Logarithmic Values of Conditional Constant and Stoichiometry of Cardiolipin (CL) and Phosphatidylserine (PS)/ Pentamethine Salt

MS	1	2	2	3	4	4	5	6	Cy5	Cy5	MT	MT
						CL						
Log(Ks[a])	n.d.[b]	5.35	-	5.10	5.80	9.90	6.80	4.89	5.30	-	5.28	-
Log(SD_{Ks}[c])	-	0.08	-	0.11	0.18	0.35	0.20	0.10	0.22	-	0.22	-
CL/MS[d]	-	1:1	-	1:1	1:1	2:1	1:1	1:1	1:1	-	1:1	-
						PS						
Log(Ks[a])	n.d.[b]	4.10	8.50	2.90	4.70	9.20	3.50	3.80	5.20	10.40	5.11	9.61
Log(SD_{Ks}[c])	-	0.27	0.43	0.30	0.35	0.27	0.16	0.30	0.23	0.63	0.22	0.18
PS/MS[d]	-	1:1	2:1	1:1	1:1	2:1	1:1	1:1	1:1	1:2	1:1	2:1

[a]Conditional constant (*Ks*), determined in 1 mM phosphate buffered saline, pH 7.3. [b]Not determined (n.d.) since no interaction of compound **1** with cardiolipin was observed. [c]Standard deviation. [d]Complex stoichiometry (analyte: methine salt).

be an alternative to improve the photostability of cyanine dyes besides the polyfluorination reaction.[44] Not only does the γ-aryl substitution of MS increase its photostability, but the expansion of the whole aromatic system causes a red shift of emission. This may be beneficial for designing novel MS for *in vivo* imaging.

MS Selectivity for Cardiolipin. We have assessed the binding of the MS to CL and PS (phospholipid localized in inner side of cell membranes). Numerous studies demonstrated interaction of MS with membrane binding partners via charge complementarity (phosphate group and carboxylate group in the case of phosphatidylserine), or through nonspecific hydrophobic interaction and hydrogen bonds.[45−48] With the exception of the neutral merocyanine **1**, we have observed an extraordinarily high affinity of **2**−**6**, Cy5, and MT to CL (see salt **3** in Figure 3; for all, see Figure S14 and Table 3). MS with benzothiazolium units (MS **2**−**6**) displayed high CL selectivity when compared to typically used mitochondrial probes based on indolium unit (MT and Cy5) (Table 3).

The logarithmic values of conditional constant (*Ks*) for the majority of studied MS were determined for stoichiometric complex 1:1 (MS:CL) (Table 3). The values of these *Ks* were approximately 10^5. MS **4** formed also stoichiometric complex 1:2 with resulting *Ks* 1 × 10,[10] thereby indicating that the pyridine group might serve as a donor of hydrogen bond. The fact that MS **3** did not display this interaction might be explained by its higher electron density. Similar effects of hydrogen bonds were also described for the indole group of ADP/ATP carrier and phosphate group of CL.[48]

Interestingly, the affinity of our MS to PS was significantly lower (see Table 3 and Figure S15). The respective *Ks* values for our set of MS were 2 orders of magnitude lower (about 10^3). In contrast, affinities of commercial pentamethine probes (Cy5 and MT) to PS were comparable to that of CL. High CL affinity was als observed for other cationic hydrophobic compounds (e.g., NAO, adriamycin, 5-iminodaunorubicin) with 1:2 stoichiometric complex (CL:probe)[49,50] with respective values of their conditional constants of about 10^6

dx.doi.org/10.1021/bc400291f | *Bioconjugate Chem.* 2013, 24, 1445−1454

M^{-1}. For comparison, the value of conditional constant of NAO complex with PS is 4.7×10^6.[49] The high affinity of MS for CL is likely caused by the combination of two binding modes: first, hydrophobic interactions between the acyl group of CL and polyaromatic salt structure, and second, an electrostatic interaction between the cationic benzothiazolium or indolium unit and the anionic phosphate residues of CL. This interaction of benzothiazolium MS was linked to significant spectral changes. Compounds **1**−**6** aggregated in aqueous media (Supporting Information Figure S13). The spectral phase, representing aggregates of MS, decreased in the presence of CL, and new maxima between 600 and 700 nm appeared (Figure 3, Figure S14). For example, the spectral maximum of salt **3** shifted from 600 to 690 nm and its intensity was significantly improved in the presence of CL (Figure 3). The spectral features of the CL-MS complexes are very similar to those observed for monomeric salt forms in DMSO and MeOH, thereby indicating the formation of methine salt 'monomer' due to CL binding. In accordance with the discussed hypothesis, more hydrophilic MS (**5**, Cy5, and MT) displayed significantly smaller spectral differences between their aggregates and CL complex corresponding to their monomeric form, and none were observed for neutral merocyanine **1**, which lacks the positive charge essential for this type of interaction (see 1A and 1B in Figure S14).

In the presence of phosphatidylserine (PS), we have observed high similarity between spectral features of MS monomers and their phosphatidylserine complexes (Figure S15) and stoichiometric complex (Table 3). For probe **2** containing nitro group, another complex stoichiometry 2:1 (PS:MS) was also found, the formation of which likely resulted from hydrogen bonding between nitrobenzene of **2** and PS aliphatic amino group derivatives. A similar type of hydrogen bond between the aromatic nitrobenzene group and the aliphatic amino group was previously described, e.g., Novakov et al.[51] and Mukhopadhyay et al.[52] In the case of MT, the stoichiometry could be explained by nonspecific hydrophobic interaction of substituted chloromethylphenyl with PS.[45,53] The 1:2 stoichiometry (PS:MS) of the Cy5 complex with PS was probably caused by the interaction of one Cy5 molecule with the phosphate group and the other with the carboxyl group of PS. The NAO interaction with CL was described by Goormaghtigh et al.[49] The spectral phase representing NAO monomer decreased in the presence of CL, while the spectral phase representing its dimeric form increased. The spectral change of NAO was significantly smaller in the presence of PS.

MS Specificity for Mitochondria in Live Cells. In order to test the ability of cyanine dyes to bind to CL in mitochondria of living cells, salts **1**−**5** were incubated with different cell lines. An example of representative intracellular localization for salts **1**−**5** in the adherent primary cell line of chicken embryonic fibroblasts (CEF) is shown in Figure 4.

Further, it was also assayed in HeLa (human cells derived from cervical carcinoma), PC-3 (human cells derived from prostate carcinomas), PaTu (cells derived from pancreas adenocarcinomas), HEK 293T (human embryonic kidney cells), 4T1 (mouse mammary tumor cell line) [Figure S16 in Supporting Information], and U-2 OS (human cells from osteosarcoma) [Figure S17]. MS localization in suspension cancer cell lines was tested using KU-812 (cells from human chronic myeloid leukemia) and HL-60 (human promyelocytic leukemia cells, Figure S18).

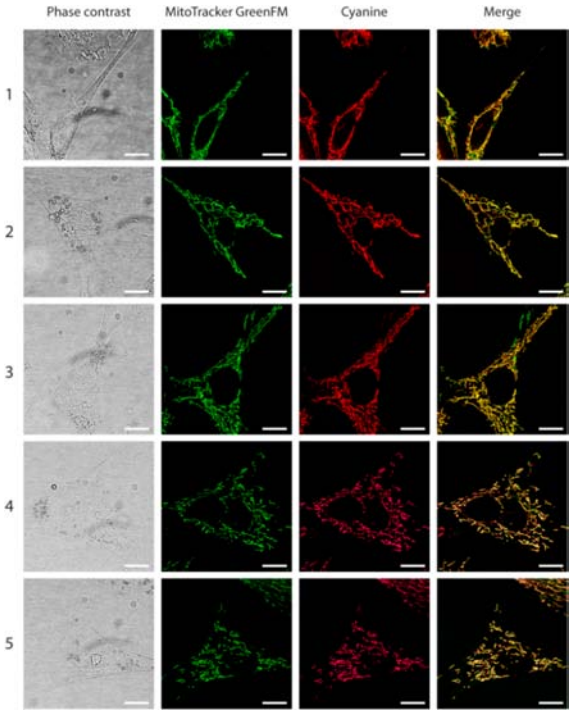

Figure 4. Pentamethine salts exclusively staining mitochondria. Fluorescent images of mitochondria stained using methine dyes **1**−**5** (in rows: concentrations of dyes 600, 15, 20, 15, 60 nM, respectively) in living primary chicken fibroblasts (CEF). In the columns (from left): phase contrast, **MTG** (100 nM), Methine salts, Merge. The scale bar represents 20 μm.

All studied compounds **1**−**5** rapidly crossed (5−10 min) the plasma membranes of living cells of all tested cell lines. To determine the actual intracellular localization of the compounds, we conducted double-staining by organelle-specific fluorescent probes. As the methine salt staining overlapped with the staining of mitochondria-specific probe MTG, we confirmed that **1**−**5** selectively accumulate in mitochondria. This ability had not been observed earlier for structures based on γ-aryl substituted methine salts. The localization efficiency was comparable for all the positively charged salts **2**−**5**, whereas the concentration of the neutral merocyanine **1** required for efficient binding to mitochondria was ca. 20 times higher. Our compounds stained mitochondria in extremely low concentrations (in the range 10−60 nM) in contrast to MTG which is usually used in 100−200 nM concentration. The minimal concentrations of MS used for efficient mitochondrial staining of the tested cell lines are summarized in Supporting Information in Table S3 and compared with commercial mitochondrial probes. Salts **2**−**5** were retained in mitochondria even after numerous washings (see video in Supporting Information) and/or in mitochondria treated using aldehyde-based fixation (Figures S19 and S20). This fidelity is caused by uniquely high affinity and selectivity of pentamethine motifs to CL (value of *Ks* $\sim 10^5$ for complex 1:1) abundantly occurring in the inner mitochondrial membrane (Table 3).

MS Specificity for Mitochondria in Fixed Cells. We have also compared the specificity and retention ability of our MS with commercial mitochondria-specific dyes upon fixation. The specificity of MT, MTG, Rhodamine 123 (R123), MitoTracker Red CM-H_2XRos (MTR), and compound **6** was tested in HeLa and U-2 OS cells fixed by 4% formaldehyde

solution. In contrast to **6**, all of the commercial dyes (MT, MTG, R123, and MTR) were dispersed in cells, though a portion of the dyes was still retained in mitochondria; we observed significant fluorescence intensity also in endoplasmic reticulum, and a noticeable signal was also apparent in cell cytoplasm and nucleus. The mitochondrial structure was not easy to resolve owing to washing out of the dyes from mitochondria. As for R123, its leakage was not surprising, since this cationic dye localizes within the inner mitochondrial membrane due to its negative potential.[54] Thus, a loss of the potential results in dye release.[54] We have observed rapid quenching during imaging of fixed cells stained with R123, which fully corresponds (quenching of R123 up to 75%[55]) to the data of Emaus et al.[55] MTG is suggested for use in live cell imaging; however, MT should be retained well in mitochondria according to published data.[56] In contrast, we have observed only partial retention of MT (more pronounced in U-2 OS cells). In comparison with our MS **2**−**5**, they were retained well in mitochondria, and their structure was clearly distinguishable. The poor retention of **1** may be caused by its different structure compared to the other tested MS. To obtain a detectable signal with this low fluorescence intensity neutral dye, it was necessary to use a high dose, likely resulting in overloading. Compound **6** acted similarly to MS **2**−**5** and it was sufficiently retained in mitochondria, though there was some signal apparent in the nuclear region as well.

Co-Localization Study of MS and Mitochondrial DNA. The localization specificity of our MS for mitochondria was further confirmed by co-staining of mitochondrial DNA (mtDNA) in living U-2 OS cells. The inner mitochondrial membrane was stained by salt **3** in living cells, as is shown in Figure 5B in red. Both the labeled mtDNA and nuclear DNA

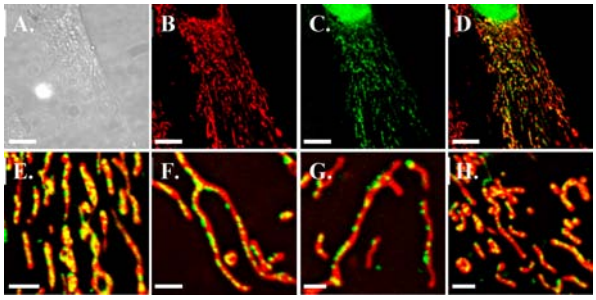

Figure 5. Staining of mitochondrial network and mtDNA in living U-2 OS cells (derived from human osteosarcoma): (A) cells in phase contrast, (B) mitochondria stained with methine salt **3** (25 nM), (C) mtDNA and nuclear DNA [pseudocolored in green], (D) merge of images B and C. In images A-D, scale bar corresponds to 20 μm. (E-H) sections of images of mtDNA merged with salt **3**. Scale bar corresponds to 4 μm in images E-H.

are depicted in Figure 5C in green. The merge image, Figure 5D, clearly shows that both dyes co-localize in the same cell compartment, mitochondria, which is more distinct in the enlarged sections of mitochondrial network (Figure 5E-H). This finding further confirmed that our novel MS localize in mitochondria.

Pentamethine Salts vs Common Mitochondrial Dyes. The main differences between the commercially available MitoTracker dyes and the novel compounds are as follows: Our dyes are derived from arylthiazolium salts and are based on pentamethine system substituted in γ-position by aryl group. Such substitution increased the stability of probes compared with those without γ-aryl substitution. The aryl substitution in the γ-position of the pentamethine chain probably increases steric hindrance of the bonds, where side arylthiazoles are connected and where the degradation process by molecular oxygen and light originates.

Moreover, the pentamethine dyes presented displayed high selectivity for mitochondria in such living cells, where staining with commercially available and widely used mitochondrial marker MTG failed. This was most pronounced in U-2 OS cells where the MTG was predominantly bound to extracellular matrix (ECM) [Figure S21 in Supporting Information], while compound **2** associated exclusively with mitochondria (Figure 6).

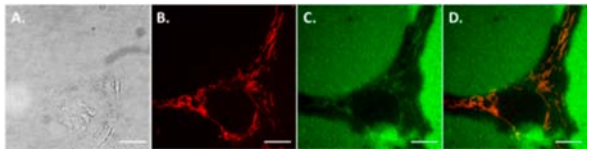

Figure 6. Superior staining of U-2 OS mitochondria with pentamethine salt **2** over **MTG** in following order: U-2 OS cells (A) in phase contrast, (B) stained with salt **2** (evident mitochondria), (C) **MTG** stains mitochondria poorly, but displays a strong unspecific background, (D) merge of B and C images. Scale bar corresponds to 20 μm.

Dark and Phototoxicity of MS. Furthermore, the dark and phototoxicity of all derivatives and commercial alternatives were tested *in vitro* in HL-60, 4T1, and U-2 OS (see growth curves in Figures S22−S23 and IC_{50} values in Tables S4 and S5 in Supporting Information). Compounds **1** and **5** exhibited neither dark nor phototoxicity. The dark and phototoxicity of MS **2**−**4** ranged in micromolar concentrations, which is above the working concentrations for live-cell microscopy. The toxicities of the tested compounds were compared with those of commercial mitochondrial markers. Although no toxicity was observed for R123 up to 10 μM concentration, for concentrations higher than 10 μM, rapid swelling of energized mitochondria was reported. The R123 cytotoxicity was ascribed to the inhibition of mitochondrial ATPase.[55] MTR displayed phototoxicity only against HL-60 cells but was well tolerated by the other tested cell lines. The dark toxicity of MT and NAO against all cell lines was similar to those of **2**−**4**. Notably, NAO appeared to be phototoxic for all the tested cell lines, particularly for HL-60.

Structure−Activity Relationship. From all the obtained results, the structure−activity relationship of the dyes can be summarized. These results showed a strong influence of cationic charge of the tested MS on their biological activity. Our synthetic methodology allows us not only to introduce increasing number of positive charges, but also to introduce selective binding groups by γ-aryl substitution and to tune up hydrophilicity/lipophilicity leading to specific intracellular localization and toxicity to cancer cells.

Biological activity of the tested MS was strongly influenced by the nature of side heteroaromate and by their charge density. We have observed efficient localization of cationic MS **2**−**5** in mitochondria of live cells even at low concentrations in contrary to the neutral merocyanine **1** (analog of charged MS **2**), for which a high concentration was required for efficient mitochondria staining. When comparing dark cytotoxicity of uncharged MS **1** and its charged analogs MS **2**−**4**, it is apparent

dx.doi.org/10.1021/bc400291f | *Bioconjugate Chem.* 2013, 24, 1445−1454

that the positive charge of MS can be one of the essential structural features to reach their biological activities (the highest toxicity was observed for MS **4**). This relation does not apply for MS **5**, which is structurally different due to the nitrogen quarternization to the second stage. Obtained results also indicated a possible correlation of hydrophilicity for MS **2**−**4** in their dark toxicity. This is in accordance with data published by Krieg et al.,[57] who found a similar cytotoxicity trend for cationic trimethine thiacarbocyanine derivatives. Salts with longer aliphatic chains were less toxic than salts with a short aliphatic chain. Nevertheless, in contrary to this hypothesis, the most hydrophilic MS **5** did not display any cytotoxicity for the cell lines used, which might again be caused by its quarternization to the second stage. Further, it might suggest that electron donor aromatic groups, e.g., pyrrole, are necessary for the MS biological activity and the loss of free electron pair strongly reduces the cytotoxicity of the dyes.

The past decade has witnessed an increase in applications of the dyes in solution, such as labeling agents. The first efforts of the use of these dyes in solution were strongly hampered by relatively low stability when compared to stability in the solid state. Degradation of polymethine dyes in solution in the presence of light and air has been a recurrent and troublesome problem over the years. The major pathway of photodecomposition involves the reaction of singlet oxygen with the chromophore. This attack results in fragmentation of the chromophore and loss of the optical properties. Bulky substituents can improve photostability of the dye as we have found in our experiments.

CONCLUSIONS

In summary, we have developed novel cell-permeable fluorescent probes for labeling and tracking mitochondria in living cells. These probes based on symmetric γ-aryl substituted pentamethine salts are specific for CL and thus the inner membrane of mitochondria in eukaryotic cells. We have described the design, synthesis, characterization, photophysical properties, and biological applications of these dyes. They are distinguished by strong fluorescence intensity, minimal fluorescence emission in aqueous environment, high photostability, low dark and phototoxicity *in vitro*, high cell-permeability, and applicability for efficient and selective staining of mitochondria of various living and fixed cell lines. Our MS possess high affinity for CL. We have shown that the performance of these dyes is superior in some aspects and comparable in others to the commonly used probes in most applications. Our γ-aryl substituted MS designed for fluorescence imaging of mitochondria might be suitable not only for studies of CL distribution and mitochondrial morphology, but also for special applications including mitochondrial physiology, pathophysiology, activity, and determination of mitochondrial mass in a cell and for monitoring of effect of new drugs on mitochondria. Besides CL and mitochondria imaging, the dyes may also be of interest for other applications such as labeling of various biomolecules. Like commonly used **Cy5**, they might be used for conjugation with primary and secondary antibodies, enzymes, DNA, RNA, aptamers, and so forth. Moreover, we must not leave out other applications for direct single molecule super-resolution microscopy, *in vivo* imaging, or for novel biomedical materials.

ASSOCIATED CONTENT

Supporting Information

Detailed experimental cell culture and microscopy procedures, spectral and characterization data of new compounds (UV−vis, absorption, fluorescence, NMR, HRMS). Crystallographic data for compound **3**. Biological data: fluorescent microscopy (images and video in live cells), CL binding, dark and phototoxicity of MS. This material is available free of charge via the Internet at http://pubs.acs.org.

AUTHOR INFORMATION

Corresponding Authors

*Tomáš Ruml: E-mail tomas.ruml@vscht.cz, tel. +420 220 443 022.

*Vladimír Král: E-mail vladimir.kral@vscht.cz, tel. +420 220 444 298.

Author Contributions

Tomáš Ruml and Vladimír Král contributed equally. All authors have given approval to the final version of the manuscript.

Notes

The authors declare no competing financial interest.

ACKNOWLEDGMENTS

This work was supported by Grant Agency of the Academy of Sciences of the Czech Republic (KAN200100801), Grant Agency of the Czech Republic (P303/11/1291, 203/09/1311), BIOMEDREG (CZ.01.05/2.1.00/01.00.30), Charles University (UNCE 204011/2012 and P24/LF1/3).

ABBREVIATIONS

MS, methine salts; STORM, stochastic optical reconstruction microscopy; CL, cardiolipin; TMRM, tetramethylrhodamine methyl ester; TMRE, tetramethylrhodamine methyl ethyl ester; DiOC6(3), [3,3-dihexyloxacarbocyanine iodide]; JC-1, [5,5′,6,6′-tetrachloro-1,1′,3,3′-tetraethylbenzimidazolylcarbocyanine iodide]; ER, endoplasmic reticulum; MTG, MitoTracker Green FM; NAO, 10-N-nonyl acridine orange; NMR, nuclear magnetic resonance; HRMS, high-resolution mass spectroscopy; DMF, dimethylformamide; DMSO, dimethylsulfoxide; MeOH, methanol; PBS, phosphate buffer saline; MT, MitoTracker Deep Red FM; *Ks*, conditional constant; PS, phosphatidylserine; ADP/ATP, adenosine diphosphate/adenosine triphosphate; CEF, embryonic chicken fibroblasts; HeLa, human cells derived from cervical carcinoma; PC-3, human cells derived from prostate carcinomas; PaTu, cells derived from pancreas adenocarcinomas; HEK 293T, human embryonic kidney cells; 4T1, mouse mammary tumor cell line; U-2 OS, human osteosarcoma cell line; KU-812, cells from human chronic myeloid leukemia; HL-60, human promyelocytic leukemia cells; R123, Rhodamine 123; MTR, MitoTracker CM-H2XRos FM; mtDNA, mitochondrial DNA.

REFERENCES

(1) Stephens, D. J., and Allan, V. J. (2003) Light microscopy techniques for life cell imaging. *Science 300*, 82−86.

(2) Chalfie, M., Tu, Y., Euskirchen, G., Ward, W. W., and Prasher, D. C. (1994) Green fluorescent protein as a marker for gene expression. *Science 263*, 802−805.

(3) Fernández-Suárez, M., and Ting, A. Y. (2008) Fluorescent probes for super-resolution imaging in living cells. *Nat. Rev. Mol. Cell. Biol. 9*, 929−943.

(4) Weissleder, R., Tung, C. H., Mahmood, U., and Bogdanov, A., Jr. (1999) In vivo imaging of tumors with protease-activated near-infrared fluorescent probes. *Nat. Biotechnol. 17*, 375−378.
(5) Mishra, A., Behera, R. K., Behera, P. K., Mishra, B. K., and Behera, G. B. (2000) Cyanines during the 1990s: a review. *Chem. Rev. 100*, 1973−2012.
(6) Sahyun, M. R. V., Sharma, D. K., and Serpone, N. (1995) Mechanisms of spectral sensitization of silver-halides − role of sensitizing dye complexation. *J. Imaging Sci. Technol. 39*, 377−385.
(7) Tani, T., Suzumoto, T., and Ohzeki, K. (1990) Energy gap dependence of efficiency of photoinduced electron transfer from cyanine dyes to silver bromide microcrystals in spectral sensitization. *J. Phys. Chem. 94*, 1298−1301.
(8) Mustroph, H., Stollenwerk, M., and Bressau, V. (2006) Current developments in optical data storage with organic dyes. *Angew. Chem., Int. Ed. 45*, 2016−2035.
(9) Lanzafame, J. M., Muenter, A. A., and Brumbaugh, D. V. (1996) The effect of J-aggregate size on photoinduced charge transfer processes for dye sensitized silver halides. *Chem. Phys. 210*, 79−89.
(10) Tuma, R. S., Baudet, M. P., Jin, X., Jones, L. J., Cheung, C. Y., Yue, S., and Singer, V. L. (1999) Characterization of SYBR Gold nucleic acid gel stain: a dye optimized for use with 300-nm ultraviolet transilluminators. *Anal. Biochem. 268*, 278−288.
(11) Giglio, S., Monis, P. T., and Saint, C. P. (2003) Demonstration of preferential binding of SYBR Green I to specific DNA fragments in real-time multiplex PCR. *Nucleic Acids Res. 31*, e136.
(12) Gibson, J. T., and Stepaniak, J. M. (1998) Examination of cyanine intercalation dyes for rapid and sensitive detection of DNA fragments by capillary electrophoresis. *J. Capillary Electrophor. 5*, 73−80.
(13) Sato, S., Tsunoda, M., Suzuki, M., Kutsuna, M., Takido-uchi, K., Shindo, M., Mizuguchi, H., Obara, H., and Ohya, H. (2009) Synthesis and spectral properties of polymethine-cyanine dye-nitroxide radical hybrid compounds for use as fluorescence probes to monitor reducing species and radicals. *Spectrochim. Acta, Part A 71*, 2030−2039.
(14) Guo, Z. Q., Chen, W. Q., and Duan, X. M. (2010) Highly selective visual detection of Cu(II) utilizing intramolecular hydrogen bond-stabilized merocyanine in aqueous buffer solution. *Org. Lett. 12*, 2202−2205.
(15) Kundu, K., Knight, S. F., Willett, N., Lee, S., Taylor, W. R., and Murthy, N. (2009) Hydrocyanines: a class of fluorescent sensors that can image reactive oxygen species in cell culture, tissue, and in vivo. *Angew. Chem., Int. Ed. Engl. 48*, 299−303.
(16) Vinatier, V., Guieu, V., Madaule, Y., Maturano, M., Payrastre, C., and Hoffmann, P. (2010) Super-oxide induced bleaching of streptocyanine dyes: Application to assay the enzymatic activity of superoxide dismutases. *Anal. Biochem. 405*, 255−259.
(17) Kawakami, M., Koya, K., Ukai, T., Tatsuta, N., Ikegawa, A., Ogawa, K., Shishidi, T., and Chen, L. B. (1998) Structure-activity of novel rhodacyanine dyes as antitumor agents. *J. Med. Chem. 41*, 130−142.
(18) Ishizawa, T., Fukushima, N., Shibahara, J., Masuda, K., Tamura, S., Aoki, T., Hasequawa, K., Beck, Y., Fukayama, M., and Kokudo, N. (2009) Real-time identification of liver cancers by using indocyanine green fluorescent imaging. *Cancer 115*, 2491−2504.
(19) Levitus, M., and Ranjit, S. (2011) Cyanine dyes in biophysical research: the photophysics of polymethine fluorescent dyes in biomolecular environments. *Q. Rev. Biophys. 44*, 123−151.
(20) Frangioni, J. V. (2003) In vivo near-infrared fluorescence imaging. *Curr. Opin. Chem. Biol. 7*, 626−634.
(21) Carreon, J. R., Stewart, K. M., Mahon, K. P., Jr., Shin, S., and Kelley, S. O. (2007) Cyanine dye conjugates as probes for live cell imaging. *Bioorg. Med. Chem. Lett. 17*, 5182−5185.
(22) Ballou, B., Ernst, L. A., and Waggoner, A. S. (2005) Fluorescence imaging tumors in vivo. *Curr. Med. Chem. 12*, 795−805.
(23) Mehranpour, A. M., Hashemnia, S., and Maghamifar, R. (2010) Synthesis and characterization of new γ−substituted pentamethine cyanine dyes. *Synth. Commun. 40*, 3594−3602.
(24) Briza, T., Kejik, Z., Cisarova, I., Kralova, J., Martasek, P., and Kral, V. (2008) Optical sensing of sulfate by polymethineium salt receptors: colorimetric sensor for heparin. *Chem. Commun. (Camb.) 28*, 1901−1903.
(25) Veverkova, L., Zaruba, K., Koukolova, J., and Kral, V. (2010) Oxoanion binding: a change of selectivity for porphyrin-alkaloid conjugates as a result of substitution pattern. *New J. Chem. 34*, 117−122.
(26) Briza, T., Kejik, Z., Vasek, P., Kralova, J., Martasek, P., Cisarova, I., and Kral, V. (2005) Chromophoric binaphthyl derivatives. *Org. Lett. 7*, 3661−3664.
(27) Briza, T., Kralova, J., Cigler, P., Kejik, Z., Pouckova, P., Vasek, P., Moserova, I., Martasek, P., and Kral, V. (2012) Combination of two chromophores: synthesis and PDT application of porphyrin-pentamethinium conjugate. *Bioorg. Med. Chem. Lett. 22*, 82−84.
(28) Daum, G. (1985) Lipids of mitochondria. *Biochim. Biophys. Acta 822*, 1−42.
(29) Nicholls, D. G., and Ward, M. W. (2000) Mitochondrial membrane potential and neuronal glutamate excitotoxicity: mortality and millivolts. *Trends Neurosci. 23*, 166−174.
(30) Perry, S. W., Norman, J. P., Barbieri, J., Brown, E. B., and Gelbard, H. A. (2011) Mitochondrial membrane potential probes and the proton gradient: a practical usage guide. *Biotechniques 50*, 98−115.
(31) Marques-Santos, L. F., Oliveira, J. G., Maia, R. C., and Rumjanek, V. M. (2003) Mitotracker green is a P-glycoprotein substrate. *Biosci. Rep. 23*, 199−212.
(32) Piccoli, C., Boffoli, D., and Capitanio, N. (2006) *Formatex microscopy book series: Current issues on multidisciplinary microscopy research and education*, University of Extremadura, Badajoz.
(33) Rottenberg, H., and Wu, S. (1998) Quantitative assay by flow cytometry of the mitochondrial membrane potential in intact cells. *Biochim. Biophys. Acta 1404*, 393−404.
(34) Mathur, A., Hong, Y., Kemp, B. K., Barrientos, A. A., and Erusalimsky, J. D. (2000) Evaluation of fluorescent dyes for the detection of mitochondrial membrane potential changes in cultured cardiomyocytes. *Cardiovasc. Res. 46*, 126−138.
(35) Haugland, R. P. (2002) *Handbook of fluorescent probes and research products*, 9th ed., Molecular Probes, Inc., Eugene, OR.
(36) Ferlini, C., and Scambia, G. (2007) Assay for apoptosis using the mitochondrial probes. Rhodamine 123 and 10-N-nonyl acridine orange. *Nat. Protocol. 2*, 3111−3114.
(37) Briza, T., Kejik, Z., Kralova, J., Martasek, P., and Kral, V. (2009) Synthesis of unsymmetric cyanine dye via merocyanine and their interaction with DNA. *Collect. Czech Chem. Commun. 74*, 1081−1090.
(38) Taroni, P., Pifferi, A., Torricelli, A., Comelli, D., and Cubeddu, R. (2003) In vivo absorption and scattering spectroscopy of biological tissues. *Photochem. Photobiol. Sci. 2*, 124−129.
(39) Bilmes, G. M., Tocho, J. O., and Braslavsky, S. E. (1989) Photophysical processes of polymethine dyes. An absorption, emission, and optoacoustic study on 3,3′-diethylthiadiacarbocyanine iodide. *J. Phys. Chem. 93*, 6696−6699.
(40) Peng, X., Yang, Z., Wang, J., Fan, J., He, Y., Song, F., Wang, B., Sun, S., Qu, J., Qi, J., and Yan, M. (2011) Fluorescence ratiometry and fluorescence lifetime imaging: using a single molecular sensor for dual mode imaging of cellular viscosity. *J. Am. Chem. Soc. 133*, 6626−6635.
(41) Sowers, A. E., and Hackenbrock, C. R. (1981) Rate of lateral diffusion of intramembrane particles: Measurement by electrophoretic displacement and rerandomization. *Proc. Natl. Acad. Sci. U.S.A. 78*, 6246−6250.
(42) Chapman, G., Henary, M., and Patonay, G. (2011) The effect of varying short-chain alkyl substitution on the molar absorptivity and quantum yield of cyanine dyes. *Anal. Chem. Insights 6*, 29−36.
(43) Toutchkine, A., Nguyen, D. V., and Hahn, K. M. (2007) Merocyanine dyes with improved photostability. *Org. Lett. 9*, 2775−2777.
(44) Renikuntla, B. R., Rose, H. C., Eldo, J., Waggoner, A. S., and Armitage, A. B. (2004) Improved photostability and fluorescence properties through polyfluorination of a cyanine dye. *Org. Lett. 6*, 909−912.

(45) Gjerde, A. U., Holmsen, H., and Nerdal, W. (2004) Chlorpromazine interaction with phosphatidylserines: A13C and 31P solid-state NMR study. *Biochim. Biophys. Acta 1682*, 28−37.
(46) Shao, C., Novakovic, V. A., Head, J. F., Seaton, B. A., and Gilbert, G. E. (2008) Crystal structure of Lactadherin C2 domain at 1.7Å resolution with mutational and computational analyses of its membrane-binding motif. *J. Biol. Chem. 283*, 7230−7241.
(47) Dahlberg, M., Marini, A., Mennucci, B., and Maliniak, A. (2010) Quantum chemical modeling of the cardiolipin headgroup. *J. Phys. Chem. A 114*, 4375−4387.
(48) Nury, H., Dahout-Gonzalez, C., Trézéguet, V., Lauquin, G., Brandolin, G., and Pebay-Peyroula, E. (2005) Structural basis for lipid-mediated interactions between mitochondrial ADP/ATP carrier monomers. *FEBS Lett. 579*, 6031−6036.
(49) Goormaghtigh, E., Huart, P., Praet, M., Brasseur, R., and Ruysschaert, J. M. (1990) Structure of the adriamycin-cardiolipin complex role in mitochondrial toxicity. *Biophys. Chem. 35*, 247−257.
(50) Petit, J. M., Maftah, A., Ratinaud, M. H., and Julien, R. (1992) 10N-nonyl acridine orange interacts with cardiolipin and allows the quantification of this phospholipid in isolated mitochondria. *Eur. J. Biochem. 209*, 267−273.
(51) Novakov, I. A., Korolkov, V. V., Pavlyuchko, A. I., Orlinson, B. S., and Gribov, L. A. (2004) Ab initio study of aniline and n-propylamine associates with nitrobenzene and m-cresol. *J. Struct. Chem. 45*, 563−569.
(52) Mukhopadhyay, P., Bharadwaj, P. K., Krishnan, A., and Das, P. K. (2004) Modulation of SHG responses via supramolecular association/dissociation between two complementary cryptands. *J. Organomet. Chem. 689*, 4877−4881.
(53) Burns, S. T., Agbodjan, A. A., and Khaledi, M. G. (2002) Characterization of solvation properties of lipid bilayer membranes in liposome electrokinetic chromatography. *J. Chromatogr. A 973*, 167−176.
(54) Chazotte, B. (2011) Labeling mitochondria with rhodamine 123. *Cold Spring Harb. Protoc. 2011*, 892−894.
(55) Emaus, R. K., Grunwald, R., and Lemasters, J. J. (1986) Rhodamine 123 as a probe of transmemebrane potential in isolated rat-liver mitochondria: spectral and metabolic properties. *Biochim. Biophys. Acta Bioenerg. 850*, 436−448.
(56) Chazotte, B. (2011) Labeling mitochondria with MitoTracker dyes. *Cold Spring Harb. Protoc. 2011*, 990−992.
(57) Krieg, M., and Bilitz, J. Z. (1996) Structurally modified trimethine thiacarbocyanine dyes. *Biochem. Pharmacol. 51*, 1461−1467.